STRUCTURAL RELAXATION IN Fe(Co)SiAlGaPCB AMORPHOUS ALLOYS

J.M. Borrego[a], J.S. Blázquez[a], S. Lozano-Pérez[b], J. S. Kim[b], C.F. Conde[a], A. Conde[a]

[a]Dpto. Física de la Materia Condensada, Instituto de Ciencia de Materiales, C.S.I.C.,

Universidad de Sevilla, P.O. Box 1065, 41080 Sevilla, Spain

[b]Department of Materials, University of Oxford, Oxford OX1 3PH, UK

Abstract

The structural relaxation of multicomponent Fe(Co)SiAlGaPCB amorphous alloys was investigated calorimetrically for annealed samples over a wide temperature range below the glass transition temperature. Upon heating, the annealed samples exhibit an endothermic reaction (enthalpy relaxation) starting around the annealing temperature and continuing over a temperature range of ~50-140 K, that it is followed by a broad exothermic reaction. Changes in the heat flow curves with annealing temperature and time were analyzed. Experimental values of enthalpic magnitudes and Curie temperature were fitted by exponential functions including two relaxation times. Values of the two relaxation times are the same for different annealing temperatures and for all the studied properties of each alloy. Saturation values of these magnitudes show a linear dependence with the inverse of the annealing temperature. Tiny domains (2-3 nm in diameter) in the matrix observed by spherical aberration corrected resolution transmission microscopy images could be ascribed to some medium-range order in the atomic structure of these quenched alloys.

I. INTRODUCTION

Since structural relaxation affects different physical, chemical and mechanical properties of amorphous alloys, the clarification of anneal-induced structural relaxation behaviour of these thermodinamically out of equilibrium alloys is important for technological applications and, also, for understanding the nature of the amorphous structure. They are metastable not only with respect to crystalline phases but also with respect to more relaxed glassy states. The structural relaxation which occurs on annealing should affect the properties of the glasses and may offer possibilities for properties optimisation.

Annealing at different temperatures causes structural relaxation in metallic glasses, which can be examined by measuring the heat flow into and out from the glasses. Upon heating for the first time, an as-quenched glass relaxes to a lower energy configuration, giving rise to an exothermic enthalpy change. In contrast, an endotherm can be observed on the calorimetric curve upon reheating a metallic glass which has been annealed at a temperature, T_a, below the glass transition temperature, T_g, or the crystallization onset temperature, T_x. It is important, therefore, to study this reversible enthalpy relaxation as it reflects an intrinsic property of the glassy phase.

Special attention has been lately paid to sub-T_g enthalpy relaxation behaviour upon low temperature annealing of non-ferrous metallic glasses such as Zr-based [1-8], Pd-based [9-12] and La-based [13]. An extensive study was made on this topic on conventional Fe-based amorphous alloys in the 80's and early 90's of the last century [14-22] but to our knowledge no systematic study on enthalpy relaxation and Curie temperature behaviour has been reported on the new bulk Fe-based magnetic multicomponent alloys.

Fe(Co)SiAlGaPCB multicomponent alloys are known to have interesting soft magnetic properties that, combined with a good glass-forming ability [23,24], makes them particularly interesting for technological applications. In this paper, the effect of composition on the annealing-induced changes in enthalpy relaxation and Curie temperature was investigated by differential scanning calorimetry.

II.   EXPERIMENTAL

Multicomponent $Fe_{70}Si_3Al_5Ga_2P_{10}C_5B_5$ and $Fe_{17}Co_{52}Si_3Al_5Ga_2P_{10}C_1B_{10}$ amorphous alloys, were prepared by arc melting under argon atmosphere. Raw materials of high purity were used; metals: 99.99%, FeC and FeB: 99.5% and FeP: 97.5%. From them, 10 mm wide and 25 μm thick ribbons were prepared by single-roller melt spinning. The values of the onset glass transition temperature, T_g, the onset crystallization temperature, T_x, and the Curie temperature, T_C, were determined by differential scanning calorimetry (DSC) (Perkin-Elmer DSC-7) under a continuous argon flow.

Prior to each test, the as-quenched samples were subjected to isothermal annealing treatment at temperatures T_a below T_g, for different annealing times. Values of temperatures are given in Table 1. After the annealing treatment, the samples were thermally scanned at 40 K/min up to 875 K, then cooled to room temperature and reheated immediately to obtain the baseline.

The microstructure of the as-cast and annealed samples was studied by high resolution transmission electron microscopy images (HRTEM) using a spherical aberration corrected JEOL-2200MCO TEM. Selected area electron diffraction patterns (SADP) were taken with a PHILIPS CM20 TEM. Both microscopes were operated at 200 kV.

III.   RESULTS AND DISCUSSION

Figure 1 shows the DSC curves for $Fe_{70}Si_3Al_5Ga_2P_{10}C_5B_5$ (a) and $Fe_{17}Co_{52}Si_3Al_5Ga_2P_{10}C_1B_{10}$ (b) alloys previously annealed at 675 K for times up to 1280 minutes. DSC curves corresponding to the as-cast samples (dashed lines) show a wide exothermic peak linked to structural relaxation towards a more stable glassy state and the endothermic peak characteristic of the glass transition. The curve corresponding to the Co-free alloys also displays the lambda shape endothermic peak characteristic of the Curie transition of the amorphous phase. The Curie endotherm of the Co-containing alloy is not observed as it falls out of the studied temperature range. The curves corresponding to the annealed samples exhibit an additional endothermic peak that starts around the annealing temperature T_a, and continues over an extended temperature range (up to 140 K) upon reheating the glass. This endothermic reaction implies that the low temperature annealing stabilizes a portion of a partial structural relaxation in the sample which upon heating destabilizes with respect to the reference state. It can also be noticed that the annealing of the samples at a constant temperature causes the progressive disappearance of the structural relaxation exothermic peak with annealing time.

The temperature dependence of the difference in heat flow between the annealed and the as-quenched samples, dH/dt(T), was analysed for several annealing temperatures, T_a. Figure 2 shows heat flow curves, dH/dt(T), (a), enthalpy change, ΔH, (b), and peak temperature, T_p, (c) data for samples of Co-containing alloy annealed at 675 K. Values of ΔH and T_p monotonically increase with annealing time and temperature up to a saturation value. For a given T_a, the experimental values were fitted by exponential functions including two relaxation times:

$$\phi(t) = \phi(0) + \sum_{i=1}^{2} \phi_i(sat)\left[1 - \exp(-t/\tau_i)\right] \tag{1}$$

where ϕ refers for ΔH or T_p. Values of $\phi(0)$ should correspond to those obtained after just reaching the corresponding annealing temperature without any further annealing time. Fitted values of $\phi(0)$ from equation (1) are in good agreement with the experimental results. Saturation values of these two magnitudes, given by:

$$\phi(sat) = \phi(0) + \sum_{i=1}^{2} \phi_i(sat) \tag{2}$$

show a linear dependence with the inverse of the annealing temperature, T_a (Figure 3).

Plots of the change of these magnitudes respect to their zero time value normalized to the saturation for each alloy, collapse in a single curve for all the considered annealing temperatures (figure 4):

$$\frac{\phi(t) - \phi(0)}{\phi(sat) - \phi(0)} = \sum_{i=1}^{2} A_i \left[1 - \exp(-t/\tau_i)\right] \tag{3}$$

and fitting results of experimental data to equation (3) for the two alloys are given in Table 2. The average characteristic times, τ_1 and τ_2, are in the order of minutes and hours, respectively, comparable to previous results on amorphous alloys (values of $\tau_1=18$ min and $\tau_2\sim18$ h were found for a Finemet alloy [25]). Both contributions are significant, as indicated by the similar values of the pre-factors A_1 and A_2 (~ 0.5). The characteristic times, τ_1 and τ_2, for Co-free alloy are higher than those found for the Co-containing alloy, related to its wider supercooled liquid region.

The Curie temperature of $Fe_{70}Si_3Al_5Ga_2P_{10}C_5B_5$ alloy shows the same behaviour than enthalpic magnitudes and follows equation (3) with the same values of relaxation times. This two relaxation times approach was previously used to describe relaxation processes for a

Finemet alloy [25], while a linear dependence with lnt of calorimetric magnitudes was found for Fe-based conventional metallic glasses [19-22,26,27]. $\Delta T_C(sat)$ values also show a linear decrease with the inverse of annealing temperature, T_a, as can be observed in figure 3c.

Enthalpic and Curie temperature relaxation results are consistent with the existence of two different processes in these alloys, which could be associated with changes in the topological (TSRO) and the chemical short range order (CSRO), respectively. The faster mechanisms would correspond to local rearrangements in the amorphous, affecting TSRO, whereas the slower processes would be related to changes in CSRO, which needs a higher atomic mobility.

An effective activation energy value for structural relaxation can be estimated from the exothermic peak temperature using the Kissinger method, in spite of the inaccuracy of the resulting value because the DSC peak is quite flat and its maximum is not well defined. The obtained values, around 1.9 ± 0.2 eV for the two studied alloys, being similar to some previously reported values of activation energy for relaxation in Fe-based alloys [25-29].

The microstructure of the as-cast and annealed samples was studied by HRTEM. Images of $Fe_{70}Si_3Al_5Ga_2P_{10}C_5B_5$ and $Fe_{17}Co_{52}Si_3Al_5Ga_2P_{10}C_1B_{10}$ as-cast samples and after annealing at 735 K for 30 minutes are shown in figures 5. Although from previous X-ray diffraction and Mössbauer results only the short-range order typical of amorphous samples was observed [30], HRTEM images from these alloys evidence tiny domains of 2-3 nm in size into the matrix. SADPs show the expected amorphous haloes but also some crystalline-like traces can be evidenced. Fast-Fourier transformation obtained from HRTEM images (right inset in figures 5) show clearly two Bragg-like rings at spacing values that should correspond to the systematic absent (100) and (111) rings of the bcc-Fe lattice. From these

observations it seems that the observed tiny domains could correspond to regions with local arrangement of atoms giving Bragg-like scattering. Atomic correlations at the nanoscale (1-3 nm) in amorphous materials is called medium-range order (MRO) to be distinguished from short-range order (first and second-nearest neighbor) and long-range order characteristic of crystals. MRO in amorphous materials of different types including metallic glasses [31-35] has been detected by means of fluctuation electron microscopy that uses spatial fluctuations in diffraction from nanoscale volume. The existence of these regions with a crystal-like order has been associated with primary crystallization, which is consistent with a quenched-in cluster model of primary crystallization [32]

In our case no evolution of these regions was found for annealed samples at temperatures below the crystallization onset and, thus, no significant effect on the relaxation studies performed can be expected.

IV. CONCLUSIONS

Annealed Fe(Co)SiAlGaPCB amorphous alloys exhibit, upon reheating, an endothermic reaction (enthalpy relaxation) that starts around the annealing temperature and continues over an extended temperature range (up to 140 K), and it is followed by a broad exothermic reaction. Changes with annealing temperature and time in the DSC curves of annealed samples with respect to the as-quenched one, analyzed in terms of enthalpy changes and peak temperature, are consistent with the existence of two relaxation processes which could be associated with changes in the topological and the chemical short range order (with relaxation times of the order of minutes and hours, respectively). Higher values are found for the Co-free alloy in accordance with its wider supercooled liquid region. The increase in Curie temperature of FeSiAlGaPCB alloy upon heating also agrees with this two relaxation

times model. Saturation values of all the studied magnitudes show a linear dependence with the inverse of the annealing temperature. An effective activation energy of 1.9 eV was estimated from the exothermic peak of the as-cast samples by the Kissinger method for both compositions. HRTEM evidences the presence of domains 2-3 nm in diameter that could indicate some medium range order in the as-cast samples with no observed evolution for annealed samples and thus, with negligible effect on the relaxation studies performed here.

ACKNOWLEDGEMENTS

References

[1]   L. Hu, Y. Yue and C. Zhang, Appl. Phys. Lett. 98 (2011) 081904.

[2]   J.C. Qiao, J.M. Pelletier, Intermetallics 19 (2011) 9.

[3]   Z. Evenson, R. Busch, J. All. Comp. 509S (2011) S38.

[4]   Y. Zhang, H. Hahn, J, Non.Cryst. Solids 355 (2009) 2616.

[5]   I. Gallino, M.B. Shah, R. Busch, Acta Mater. 55 (2007) 1367.

[6]   A. Slipenyuk, J. Eckert, Scripta Mater. 50 (2004) 39.

[7]   R. Busch and W.L. Johnson, Appl. Phys. Lett. 72 (1998) 2695.

[8]   M. Mao, Z. Altounian, J. Non-Cryst. Solids 205-207 (1996) 633.

[9]   M. Kohda, O. Haruyama, T. Ohkubo and T. Egami. Phys. Rev. B 81 (2010) 092203.

[10]   O. Haruyama, H. Sakagami, N. Nishiyama, A. Inoue, Mat. Sci. Eng. A 449-451
(2007) 497.

[11]   O. Haruyama and A. Inoue, Appl. Phys. Lett. 88 (2006) 131906.

[12]   G.J. Fan, J.F. Löffler, R.K. Wunderlich and H.J. Fecht, Acta Mater. 52 (2004) 667.

[13]   T. Zhang, F. Ye, Y.L. Wang, and J.P. Lin. Metal. Mater. Trans. A 30 (2008) 1953.

[14]   T-H Noh, A. Inoue, H. Fujimori and T. Masumoto, J. Non-Cryst. Solids 152 (1993)
212.

[15]   T-H Noh, A. Inoue, H. Fujimori, T. Masumoto and I.K. Kang, J. Non-Cryst. Solids
110 (1989) 190.

[16]   A. Inoue, T. Masumoto and H.S. Chen, J. Non-Cryst. Solids 83 (1986) 297.

[17]   T. Komatsu, S. Sato and K. Matusita, Acta Metall. 34 (1986) 1899.

[18]   T. Komatsu, K. Matusita and R. Yokota, J. Mater. Sci. 20 (1985) 3271.

[19]   H.S. Chen, A. Inoue and T. Masumoto, J. Mater. Sci. 20 (1985) 2417.

[20]   A. Inoue, T. Masumoto and H.S. Chen, J. Mater. Sci. 19 (1984) 3953.

[21]   H.S. Chen, J. Appl. Phys. 52 (1981) 1868.

[22]   Y.N. Chen and T. Egami, J. Appl. Phys. 50 (1979) 7615.

[23]   J. M. Borrego, A. Conde, S. Roth, J. Eckert, J. Appl. Phys. 92 (2002) 2073.

[24]   V. Franco, J.M. Borrego, A. Conde, S. Roth, Appl. Phys. Lett. 88 (2006) 132509.

[25]   J.S. Blázquez, S. Lozano-Pérez, A. Conde, Matt. Lett. 45 (2000) 246.

[26]   C.F. Conde, H. Miranda, A. Conde, Matt. Lett. 10 (1991) 501-503.

[27]   C.F. Conde, A. Cnde. Proc. III Int. Workshop on Non-Crystalline Solids, Ed. World
Scientific (1992) 261-264.

[28]   J. Zhu, M.T. Clavaguera-Mora, N. Clavaguera, Appl. Phys. Lett. 70 (1997) 1709.

[29]   J.M. Borrego, C.F. Conde and A. Conde, Mater. Sci. Eng. A 304-306 (2001) 491

[30]   J. M. Borrego, C. F. Conde, A. Conde, S. Roth, J. Eckert and J.M. Greneche, J. Appl. Phys. 95 (2004) 4151.

[31]   T.C. Hufnagel, C. Fan, R.T. Ott, J. Li, S. Brennan, Intermetallics 10 (2002) 1163-1166.

[32]   W.G. Stratton, J. Hamann, J.H. Perepezko, P.M. Voyles, Apl. Phys. Lett. (2005) 86 (14)

[33]   W.G. Stratton, J. Hamann, J.H. Perepezko, P.M. Voyles, Intermetallics 14 (2006) 1061-1065.

[34]   G. Li, K.B. Borisenko, Y. Chen, D. Nguyen-Manh, E. Ma, D.J.H. Cockayne, Acta Mater. 57 (2009) 804-811).

[35]   A. Yan, T. Sun, K.B. Borisenko, D. B. Buchholz, R. P. H. Chang, A. I. Kirkland, and V. P. Dravid, J. Appl. Phys. 112, 054907 (2012)

Table 1

Alloy	$Fe_{70}Si_3Al_5Ga_2P_{10}C_5B_5$	$Fe_{17}Co_{52}Si_3Al_5Ga_2P_{10}C_1B_{10}$
T_g (K) ±5	755	782
T_x (K) ±1	809	828
T_C (K) ±3	568	373

Table 2

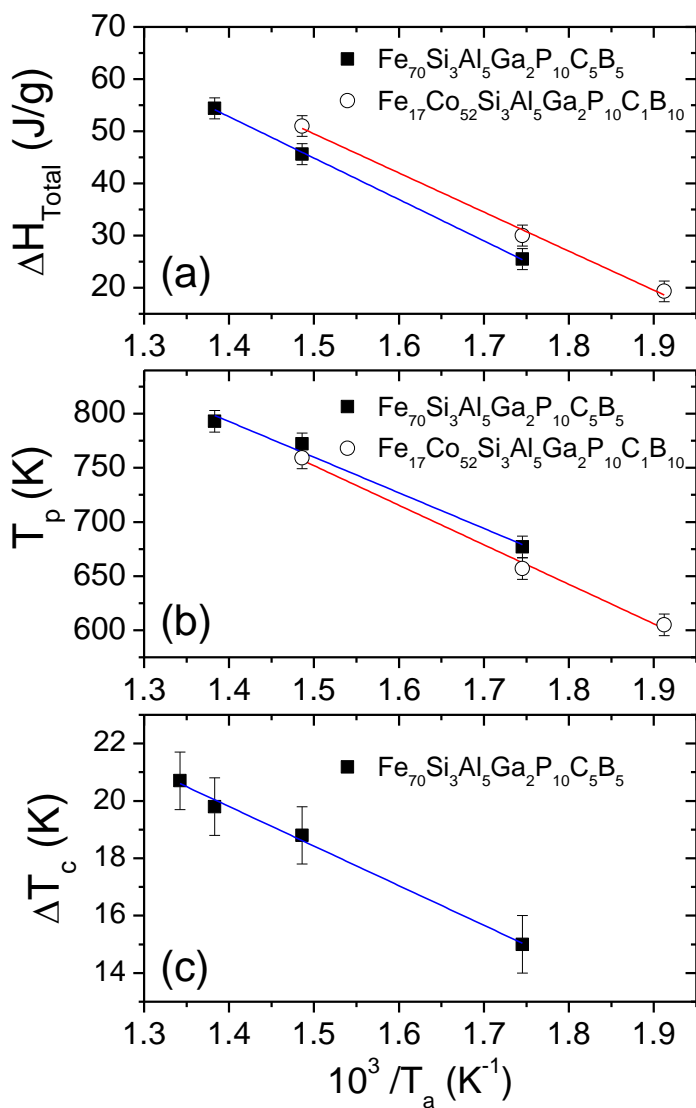| Alloy	τ_1 (min)	A_1	τ_2 (h)	A_2
$Fe_{70}Si_3Al_5Ga_2P_{10}C_5B_5$	25(5)	0.50(7)	5(1)	0.49(7)
$Fe_{17}Co_{52}Si_3Al_5Ga_2P_{10}C_1B_{10}$	6(2)	0.44(3)	2.5(5)	0.53 (2)

Figure 1
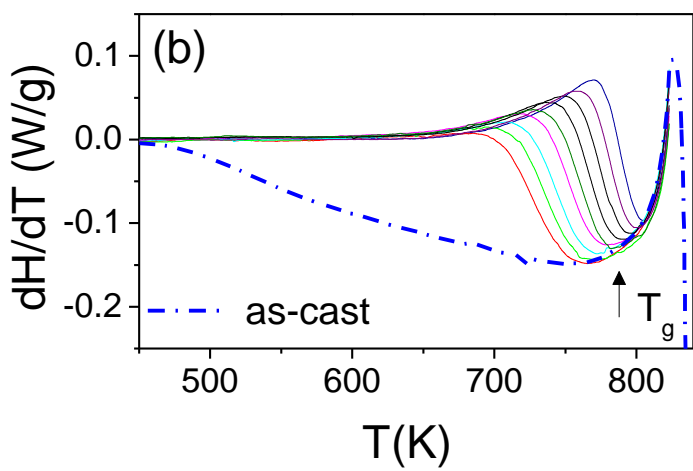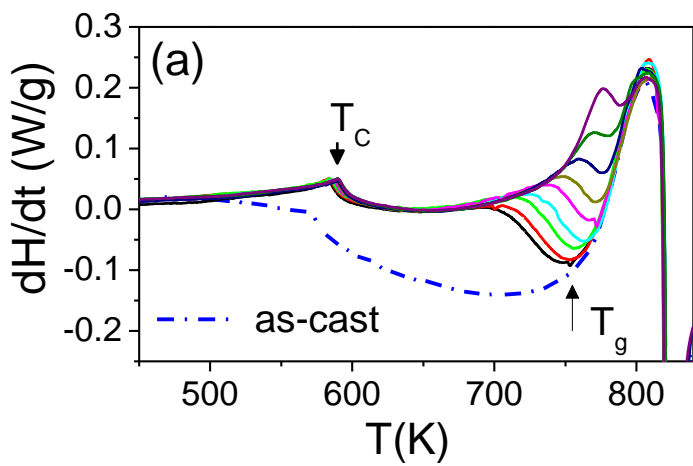
Figure 2
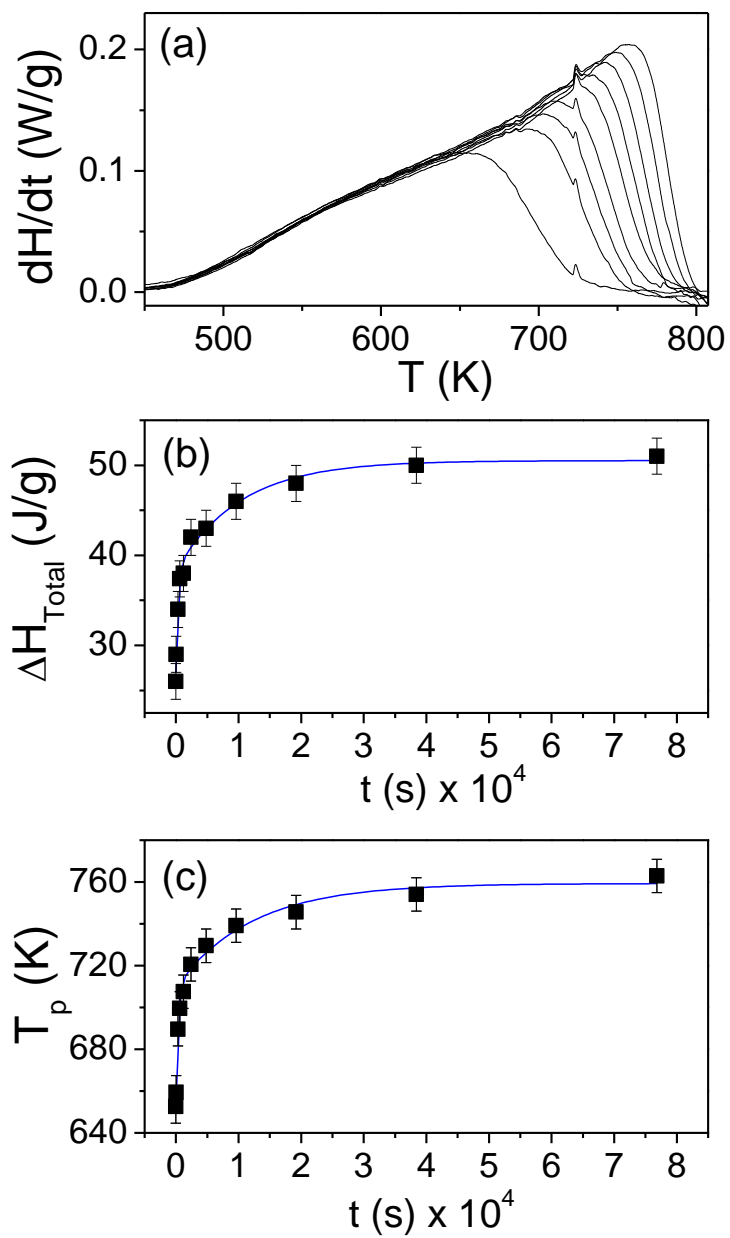
Figure 3 (2ª version)

Figure 4

Figure 5